

The JT-60 Tokamak Machine

Y. Iso, M. Ohta

*Japan Atomic Energy Research Institute,
Fusion Research and Development Center, Tokai-mura, Naka-gun, Ibaraki-ken, Japan*

Summary

JT-60 is a large tokamak experimental device under construction at JAERI with main device parameters of $R=3.0\text{m}$, $a=0.95\text{m}$, $B_t=45\text{kG}$, and $I_p=2.7\text{MA}$. Its basic aim is to produce and confine hydrogen plasmas of temperatures in a multi-keV range and of confinement times comparable to a second, and to study its plasma-physics properties as well as engineering problems associated with them.

The JT-60 tokamak machine is mainly composed of a vacuum vessel, toroidal field (TF) coils, poloidal field (PF) coils, and support structures.

The vacuum vessel is a high vacuum toroidal chamber with an egg-shaped crosssection, consisting of sectorial rigid rings and parallel bellows made from Inconel 625. It is baked out at a maximum temperature up to 500°C . Several kinds of first walls made from molybdenum are bolt-jointed to the vacuum vessel for its protection. The vacuum vessel is almost completely finished with design and is deeply into manufacturing.

The TF coil system consists of 18 unit coils located around a torus axis at regular intervals. The unit coil composed of two pancakes are wedge-shaped at the section close to a torus axis and encased in a high-manganese non-magnetic steel case. Fabrication of the TF coils will be finished in May 1981.

The PF coils are composed of ohmic heating coils, vertical field coils, horizontal field coils, and quadrupole field coils located inside the TF coil bore and outside the vacuum vessel, and magnetic limiter coils placed in the vacuum vessel. Its mechanical and thermal design is almost completed and the bending and machining have already started.

Support structures are composed of the upper and lower support structures, support columns of the vacuum vessel, and central column made from high-manganese non-magnetic steel. The structural analysis was completed including a seismic analysis and the fabrication is now in progress.

The first plasma is expected to be produced in October 1984.

1. Introduction

JT-60 is one of the four large tokamaks now under construction in the world, aiming at the break-even plasma condition. It has been developed since 1975 by Japan Atomic Energy Research Institute and some of its main components are almost fabricated ready for installation.

Although it is an experimental device for studying plasma physics problems, it also has various unique characteristics in the mechanical and engineering point of view.

- a) It has very large scale compared with existing tokamak machines. Combined with the complexity of torus configuration, it gives us new structural problems in designing, fabricating and installation.
- b) Large tokamaks are also characterized as heavy electrical machines which correspond to a very large amount of peak electric current and power. Consequently, it is subject to the multiple, strong electromagnetic forces together with the thermal loads due to the operation.
- c) These new type of structural requirements are far beyond the conventional technique, and need a lot of new development work to be done.

However it should be recognized that these problems are almost the same as in tokamak reactors in future, and the experiences in JT-60 construction should be a necessary step toward the fusion reactor development as a big milestone in engineering.

Table 1 shows main parameters of the JT-60. Plasma major and minor radii are 3m and 0.95m, respectively, and a toroidal field intensity is 45kG at the plasma axis of 3m. The expected ion temperature of $5 \sim 10$ keV is obtained by the heating power of 30MW by neutral beam heatings and 10MW by radiofrequency heatings. The product of density and confinement time is expected to be $(2 \sim 10) \times 10^{13}$ sec/cm³. Figure 1 shows the bird's eye view of the JT-60 machine.

In the present paper are discussed main components of the JT-60 machine, that is, a vacuum vessel, toroidal field (TF) coils, poloidal field (PF) coils and support structures.

2. Vacuum Vessel

The vacuum vessel with a non-circular crosssection is composed of 8 sectorial rigid rings 65mm thick and 8 parallel U-shaped bellows 2.5mm thick, 20mm pitch, and 70mm high. They are made from Inconel 625 and are connected alternately by welding. Its vacuum pressure is expected to be less than 10^{-8} torr after bake-out up to 500°C. A one-turn electric resistance is required to be more than 1.3mΩ. Figure 2 shows the crosssection of the vacuum vessel and some components of first walls placed inside the vessel. Seventeen lines of toroidal fixed limiters, protection plates from the bombardment of ripple trapped fast ions, magnetic limiter plates, local poloidal limiters are made from molybdenum 20mm thick. Protection plates of neutral beam shine-through and liners covering magnetic limiter coils are also made from molybdenum 5mm thick. All of the first wall are bolt-jointed to the vacuum vessel. Heaters and cooling channels are attached outside the vessel and thermal insulation layers cover the whole vessel and ports.

Mechanical loads on the vessel come from atmospheric pressure, thermal expansion due to 500°C bake-out and electromagnetic forces caused by the interaction between magnetic fields and eddy currents induced at a plasma build-up phase and plasma disruptions. The estimation of the eddy currents is made separately by using two numerical codes of finite element

circuit code EDDYTORUS [1] and current vector potential method [2]. The applicability of both codes to the JT-60 design is confirmed by comparing the calculated results with the experimental ones using small test models.

The design has been done assuming plasma build-up failure with 5% shots of total and 1 msec major plasma disruptions with 1000 shots. The maximum calculated loop current of 1.4MA and the saddle-like current of 220kA are found at the 1msec disruption. Figure 3 shows the eddy current distribution induced on the vacuum vessel in the above case.

The stress analysis by the finite element method (FEM) has been done in such a way that at first the bellows are replaced with an orthotropic plate having the same rigidity as that of the bellows and then the stress of the whole torus consisting of isotropic rigid rings and the orthotropic plates is computed by FEM and lastly the stress of the local part of bellows is analyzed by giving the calculated results of the whole torus to the boundary conditions of the local analysis. The calculation is verified with a good agreement with the experiments using one-fifth scaled and full scaled models of the vessel [3].

The maximum stress intensity of 40kg/mm^2 including a thermal stress at the 1msec disruption is observed on the top of bellows close to rigid rings. Stresses of the same point due to the thermal expansion and atmospheric pressure are 18kg/mm^2 and 1kg/mm^2 , respectively. Calculated stresses of the vessel are lower than the allowable stress of Inconel 625 given in conformity to ASME code, where the guaranteed 0.2% yield and ultimate stresses of 2.5mm thick plates are 42.2kg/mm^2 and 84.4kg/mm^2 , respectively. Fatigue strength and brittleness at higher temperatures are also taken into account, comparing design values with experimentally obtained data of its mother material and welded ones [4]. The dynamic response of the vessel due to the electromagnetic force at the disruption is discussed in detail [5]. Structural integrity is confirmed from the viewpoint of fatigue analysis, taking the transient response and free vibration after the impulse into consideration.

The estimation of eddy currents of the first walls is done by the other code EDDYARBT [6]. The maximum changing rate of the magnetic field at the disruption is found to be 7kG/msec on the liner covering the magnetic limiter coil.

The allowable stress of molybdenum is decided from the measured data of ultimate strength, 0.2% yield stress, elongation and fatigue curves up to 800°C. The aspect ratio of rectangular first wall is designed from the discussion of the above data and the calculated stress.

The design of heat removal is based on the thermal load in controlled plasma discharges obtained from the DIVA scaling in JAERI [7]. The load for 10sec discharges is estimated to be $1\sim 2\text{kW/cm}^2$ on the fixed limiter, in the order of 10W/cm^2 on liners and 400W/cm^2 on the magnetic limiter plates. The magnetic limiter plate and local poloidal limiters are provided with nitrogen gas cooling channels. The other first walls are cooled down by radiation and thermal conduction for the repetition time of 10min. The major causes for concern are the disruptive loss of plasma energy, neutral beam shine-through and runaway electron loads. It is difficult to estimate the thermal load at the disruption because of a serious lack of information of the energy dissipation duration and heat-deposited area. In the case of large neutral beam shine-through, thermocouple or infra-red camera signals are fed back to switch off the beam. The runaway electron load in the order of 100kW/cm^2 is afraid to lead the first wall to be melt.

The low Z coating on the first walls has been discussed and several tests are under way using small test specimens made by some coating techniques. The candidate materials are C,

SiC, and TiC and TiN coated on molybdenum and Inconel 625. The coating technique before assembly will be developed in fiscal 1981 using full scaled fixed limiters and liners, and final decision will be made in March 1982. In-site coating technique is also being developed and is expected to be established before a first plasma production.

Concerning the status of fabrication, the materials of the rigid ring and bellows have been delivered to works and the vessel is deeply into manufacturing. Photo 1 shows the shaped rigid ring of the vacuum vessel.

3. Toroidal Field Coil

The TF coils system consists of 18 unit coils located around the torus axis at regular intervals. The unit coil is wedge-shaped at the section close to the torus axis because of the necessity of a lower aspect ratio of plasma and is encased in a high-manganese non-magnetic steel case. Photo 2 shows a fabricated TF unit coil. The coils with a major radius of 3.32m and an inner bore of 3.9m produce the field intensity of 45kG at a plasma axis of 3m.

The hoop force of 2.7×10^5 ton around a minor axis and the centripetal force of 1.0×10^5 ton toward the torus axis are withstood by copper conductors, high-manganese steel and a center column located at the torus axis. The twisting moment of 2.6×10^4 ton·m caused by the interaction of TF coil current with the poloidal field is withstood by building walls through the trusses extended from an upper support structure.

The unit coil is composed of 2 pancakes, one of which is wounded into 36 layers. The conductor is oxygen free high tension copper (OFC) containing 0.2% silver with 40% cold rolling ratio. The thickness of each turn is not uniform in order to equalize the temperature rise of each turn in the wedge-shaped crosssection. Each turn is provided with a water cooling channel. The layer insulator 1mm thick is made of a main insulator of a polyamid paper and two tolerance absorbers of non-woven glass fiber placed on each side of the main insulator. They are pre-pregnated with an epoxy resin and kept in a semi-cure stage. The ground insulator consists of a main insulation layer of mica and a protection layer of glass fiber reinforced plastics.

The 0.2% yield strength and ultimate strength are guaranteed to be 65kg/mm² and 90kg/mm² in the steel and 32.5kg/mm² and 33.0kg/mm² in OFC. On the other hand, the maximum stress intensities of 17kg/mm² and 46kg/mm² are computed in the conductor and case, respectively. The stress intensity of brazed joint does not exceed 5kg/mm². The ratios of 0.2% yield stress to primary membrane stress are 2.0 in the wedge-shaped conductor, 1.5 in the brazed joint, and 1.7 in the case, respectively. The safety margins of fatigue strength, on the other hand, are more than 1.5 in the wedge-shaped conductor, 3.1 in the brazed joint and 1.5 in the case, respectively.

A two-dimensional code is used to calculate the temperature distribution. The maximum temperature in the conductor rises up to 120°C in the outer turn of wedge-shaped crosssection.

The fabrication of the TF coil is almost completely finished. The mechanical and thermal integrity was confirmed in the test where the mechanical loads simulating the actual were put on the first fabricated unit coil by using oil jacks [8]. Figure 4 shows the comparison between the calculated stress and the measured in the above test.

4. Poloidal Field Coil

The PF coils are composed of ohmic heating (OH) coils, vertical field (V) coils, horizontal field (H) coils, and quadrupole field (Q) coils placed inside the TF coil bore and outside the vacuum vessel as well, and magnetic limiter (M) coils located in the vacuum

vessel. The former four are supported by support frames made from high-manganese non-magnetic steel. The latter is encased in a coil can composed of rings and bellows, which are connected alternately by welding because of vacuum tightness, and are fixed to the vacuum vessel.

Table 2 summarizes the specification of the PF coil. The OH coils of 60 turns are capable of inducing the plasma current up to 2.7MA for 0.1sec and maintaining the maximum plasma current for about 5sec. The maximum field capability of V coils is 3.3kG at the major radius of 3m. The V coil design provides for the variable vertical field curvature index 0 to 1 with the superposition of quadrupole field. The horizontal field is designed to be capable of 200G at the major radius of 3m. The design loading condition of the M coil composed of a main coil and two sub-coils is based on the plasma current of 2.1MA.

The conductors and insulators of PF coils are same as those of the TF coil. The maximum calculated membrane stress P_m and bending stress P_b of the copper are calculated to be 11kg/mm^2 and 7kg/mm^2 , respectively. The safety margin of the PF coil is in the same level as that of the TF coil from the viewpoint of mechanical and fatigue strengths. The maximum coil temperature of 150°C in the connection welded at the assembly does not exceed the allowable temperature of the coil insulator.

The materials of conductors and insulators have already been delivered to works and the bending and machining are now in progress.

5. Support Structure

Support structures are composed of the upper and lower support structures, support columns of the vacuum vessel, and the central column made from high-manganese non-magnetic steel, as shown in Fig. 5. Each component is electrically insulated with each other in order to reduce eddy currents. The support structure supports the machine weighing about 5000 ton and also withstands various electromagnetic forces on the coils and vacuum vessel, and earthquakes with the ground acceleration of 200 gal. The stress analysis of each component and seismic analysis [9] of the JT-60 machine made it clear to confirm the machine integrity of mechanical structure.

The fabrication of support structures will be completely finished in May 1981.

The JT-60 has developed the new analytical methods and engineering techniques in designing, fabricating, and assembling. The fabrication of JT-60 machine components is now satisfactorily in progress. The assembly of JT-60 machine itself will be initiated in early 1983 and the first plasma is expected to be produced in October 1984.

References

- /1/ KAMEARI, A., SUZUKI, Y., "Eddy Current Analysis by the Finite Element Circuit Method", JAERI-M 7120 (1977).
- /2/ TAKIZAWA, T., et al., "An Eddy Current Test on a Tokamak Vacuum Vessel Model", 11th Symposium on Fusion Technology, Oxford, United Kingdom, September 15-19, 1980.
- /3/ TAKATSU, H., et al., "Stress Analysis of Vacuum Vessel in JT-60", 7th Symposium on Engineering Problems of Fusion Research, Knoxville, October 25-28, 1977.

- /4/ YAMAMOTO, M., et al., "Research and Development of the JAERI Large Tokamak (JT-60), (III) Vacuum Vessel", J. At. Energy Soc. Japan, 20, 258 (1978).
- /5/ UDOGUCHI, T., et al., "Dynamic Response Analysis on the Vacuum Vessel of JT-60 against the Saddle-like Electromagnetic Forces", 11th Symposium on Fusion Technology, Oxford, United Kingdom, September 15-19, 1980.
- /6/ NINOMIYA, H., et al., "Studies of Eddy Currents in JT-60", 8th Symposium on Engineering Problems of Fusion Research, San Francisco, November 13-16, 1979.
- /7/ DIVA Group, "Divertor Experiment in DIVA", Nuclear Fusion 18 1619 (1978).
- /8/ OHKUBO, M., et al., "A Reliability Test on a Toroidal Field Coil by imposing Force and Heat simulating the Actual Load", 11th Symposium on Fusion Technology, Oxford, United Kingdom, September 15-19, 1980.
- /9/ TAKATSU, H., et al., "Seismic Analysis of the JT-60", 8th Symposium on Engineering Problems of Fusion Research, San Francisco, November 13-16, 1979.



Photo 1. Shaped sectorial rigid ring of the vacuum vessel.

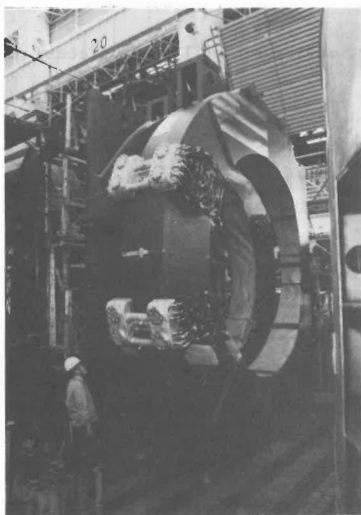


Photo 2 Fabricated TF unit coil.

Table 1 Main Parameters of JT-60

Parameter	Design Values
Major radius	3 m
Minor radius	0.95 m
Toroidal field	45 kG
Plasma current	2.7 MA
Discharge duration	5 sec
Repetition time	10 min
Input power (NBI)	30 MW
Input power (RF)	10 MW
Expected ion temperature	5 - 10 keV
Expected confinement time	0.2 - 1.0 sec

Table 2 Poloidal Field Coil Specifications

Parameter	OH coil	V coil	H coil	Q coil	M coil
Ampere turns (MAT)	5.5	3.68	0.24	0.90	1.51
Total turns	60	64	12	36	16
Max. current (kA)	91.7	57.5	20	25	94.4
Inductance (mH)	8.3	9.7	0.44	2.22	0.87
Resistance* (at 75°C) (mΩ)	4.6	12.1	4.1	13.0	3.2
Time constant (sec)	1.8	0.80	0.11	0.17	0.27
I^2R (MW)	38.7	40.0	1.6	8.1	28.5
$LI^2/2$ (MJ)	34.9	16.0	0.09	0.69	3.9
Equivalent square wave pulse length (sec)	8	6	7	7	7

* not including feeders

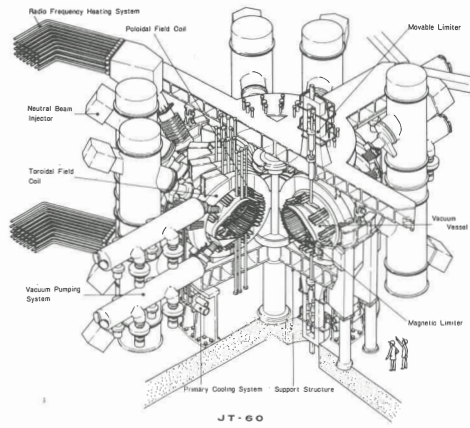


Fig. 1. Bird's eye view of the JT-60 machine.

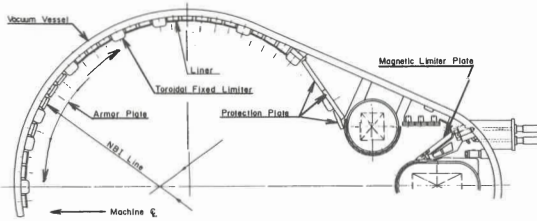


Fig. 2. Cross section of the vacuum vessel and the first walls.

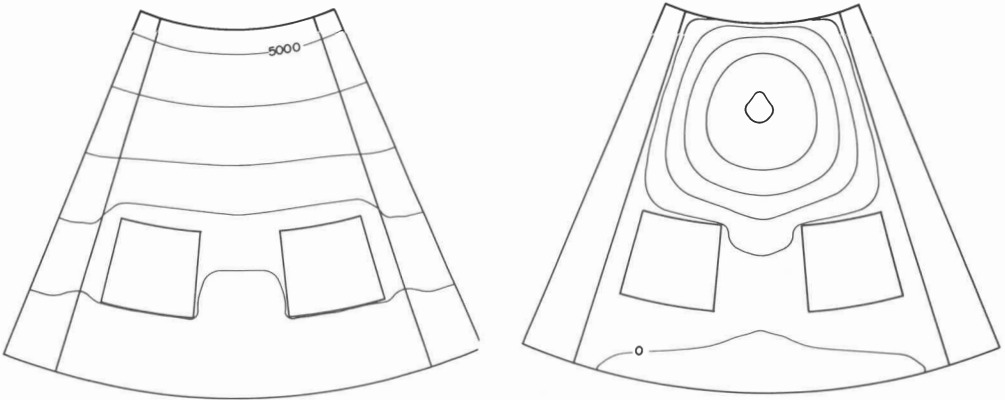


Fig. 3. Eddy current distributions on the 45° sectorial vacuum vessel with two port holes in the case of 1 msec disruption. (a) at 1 msec after the disruption and (b) at 13 msec after the disruption.

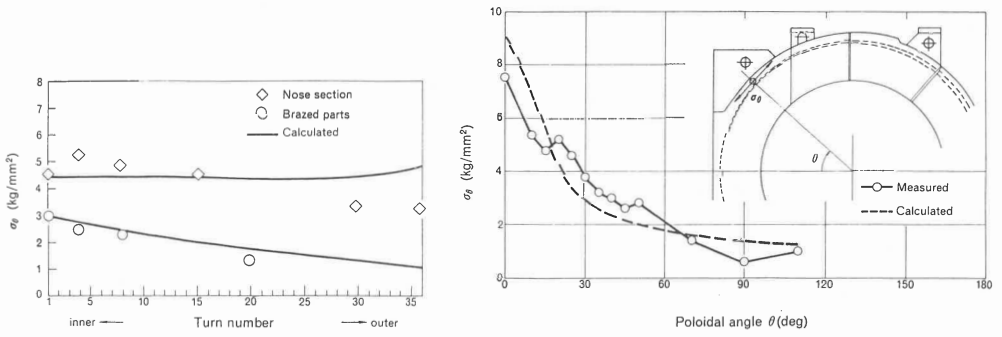


Fig. 4. Comparison between the calculated stress and the experimental result of the TF coil. (a) conductor stresses and (b) high manganese steel case stresses.

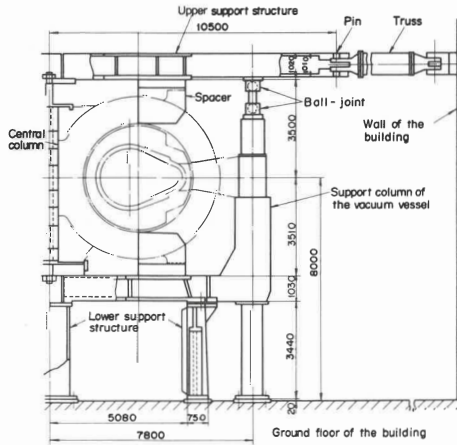


Fig. 5. Schematic view of the support structure.

